The ISME Journal (2021) 15:3084–3093
https://doi.org/10.1038/s41396-021-00990-2

ARTICLE

Stainless steel corrosion via direct iron-to-microbe electron transfer by *Geobacter* species

Hai-Yan Tang[1,2,3,4] · Chuntian Yang[1,2] · Toshiyuki Ueki[4] · Conor C. Pittman[4] · Dake Xu[1,2,4,5] · Trevor L. Woodard[4] · Dawn E. Holmes[4] · Tingyue Gu[6] · Fuhui Wang[1,2] · Derek R. Lovley[4,5]

Received: 19 June 2020 / Revised: 28 March 2021 / Accepted: 14 April 2021 / Published online: 10 May 2021

Abstract

Microbial corrosion of iron-based materials is a substantial economic problem. A mechanistic understanding is required to develop mitigation strategies, but previous mechanistic studies have been limited to investigations with relatively pure Fe(0), which is not a common structural material. We report here that the mechanism for microbial corrosion of stainless steel, the metal of choice for many actual applications, can be significantly different from that for Fe(0). Although H_2 is often an intermediary electron carrier between the metal and microbes during Fe(0) corrosion, we found that H_2 is not abiotically produced from stainless steel, making this corrosion mechanism unlikely. *Geobacter sulfurreducens* and *Geobacter metallireducens,* electrotrophs that are known to directly accept electrons from other microbes or electrodes, extracted electrons from stainless steel via direct iron-to-microbe electron transfer. Genetic modification to prevent H_2 consumption did not negatively impact on stainless steel corrosion. Corrosion was inhibited when genes for outer-surface cytochromes that are key electrical contacts were deleted. These results indicate that a common model of microbial Fe(0) corrosion by hydrogenase-positive microbes, in which H_2 serves as an intermediary electron carrier between the metal surface and the microbe, may not apply to the microbial corrosion of stainless steel. However, direct iron-to-microbe electron transfer is a feasible route for stainless steel corrosion.

Introduction

Understanding of the mechanisms for iron-to-microbe electron transfer could lead to improved strategies to reduce the estimated 500 billion dollars of annual damage [1] associated with microbially enhanced corrosion. Corrosion develops when metallic iron, Fe(0), is oxidized to Fe(II), with a release of electrons [2, 3]. Although the role for microorganisms in iron corrosion has been recognized for over 100 years [4], the mechanisms for electron exchange between Fe(0) and microorganisms are still poorly understood.

Economically important metal surfaces, such as the interior of oil pipelines and fuel storage tanks, as well as buried pilings and other structures, are usually anaerobic. Anaerobic mechanisms for iron metal corrosion have typically been studied with pure Fe(0). H_2 can be an important electron carrier that shuttles electrons from Fe(0) to microorganisms [5–9]. Even in the absence of microorganisms, electrons

These authors contributed equally: Hai-Yan Tang, Chuntian Yang

Supplementary information The online version contains supplementary material available at https://doi.org/10.1038/s41396-021-00990-2.

✉ Dake Xu
xudake@mail.neu.edu.cn

[1] Shenyang National Laboratory for Materials Science, Northeastern University, Shenyang, China

[2] State Key Laboratory of Rolling and Automation, Northeastern University, Shenyang, China

[3] Jiangsu Provincial Key Lab for Organic Solid Waste Utilization, Jiangsu Collaborative Innovation Center for Solid Organic Waste Resource Utilization, Educational Ministry Engineering Center of Resource-saving Fertilizers, Nanjing Agricultural University, Nanjing, China

[4] Department of Microbiology, University of Massachusetts Amherst, Amherst, MA, USA

[5] Electrobiomaterials Institute, Key Laboratory for Anisotropy and Texture of Materials (Ministry of Education), Northeastern University, Shenyang, China

[6] Department of Chemical and Biomolecular Engineering, Ohio University, Athens, OH, USA

derived from Fe(0) can reduce H^+ to H_2:

$$Fe^0 + 2H^+ \rightarrow Fe^{2+} + H_2 \quad (1)$$

Various anaerobic microorganisms can consume the H_2 released from Fe(0), coupling H_2 oxidation to the reduction of electron acceptors other than oxygen [7–10].

Direct iron-to-microbe electron transfer, eliminating H_2 as an intermediary electron carrier between Fe(0) and microorganisms, is a potential alternative for microbially catalyzed corrosion [11–14]. The concept of direct iron-to-microbe electron transfer is an extension of the general concept of electrotrophy, in which anaerobic microorganisms harvest energy to support growth by directly accepting electrons from other microbial cells or electrodes [15]. Direct microbial electron uptake from Fe(0) has been proposed for a diversity of sulfate-reducing, methane-producing, and acetogenic microorganisms [8, 12, 13, 16–22]. However, all of these microbes also have the ability to consume H_2, raising the possibility that, rather than relying on electrotrophy, these microbes accelerate corrosion because they are effective in enzymatically accelerating H_2 production and/or attaching to Fe(0) and consuming H_2 as it is released at the surface [5, 10, 11, 23].

In order to rigorously rule out the potential for H_2 serving as an intermediary electron carrier in Fe(0) corrosion, it is necessary to evaluate corrosion with strains that cannot use H_2 [23]. This was accomplished in studies with a strain of *Geobacter sulfurreducens* genetically modified to prevent H_2 consumption [11]. *G. sulfurreducens* strain ACL_{HF} is unable to utilize H_2 or formate because genes necessary for H_2 and formate oxidation have been eliminated [11]. Strain ACL_{HF} grew on the surface of Fe(0), which served as the sole electron donor for the energy-yielding anaerobic respiration with reduction of fumarate to succinate [11]. H_2 abiotically produced from Fe(0) in the cultures was not consumed. Deletion of the gene for the outer-surface multi-heme *c*-type cytochromes OmcS or OmcZ inhibited growth on Fe(0) [11]. The capacity for growth on Fe(0) was restored when the genes for these cytochromes were reintroduced. These studies suggested that direct electron uptake from Fe(0), mediated by outer-surface *c*-type cytochromes, is possible and demonstrated that *G. sulfurreducens* is an effective model microbe for determining whether direct iron-to microbe electron transfer is feasible [11].

However, under the same conditions, the parent strain of strain ACL_{HF}, strain ACL, which is able to use H_2, grew primarily on H_2 released from Fe(0) [11]. This finding suggested that, although direct iron-to-microbe electron transfer is possible, microbially induced Fe(0) corrosion may proceed with H_2 as an intermediary electron carrier in open environments where diverse H_2-consuming microbes are found.

Pure Fe(0) is a convenient well-defined substrate for mechanistic studies, but iron is amended with other metals for most practical applications. For example, stainless steel (type 316L) is the metal of choice for many oilfield devices and marine applications [24]. Stainless steel contains a minimum of 11% chromium. As the outer surface corrodes, a layer of chromium oxides forms, providing protection to the underlying matrix from direct contact with the external environment [25]. Thus, the mechanisms for microbial electron extraction from stainless steel might be significantly different from that for pure Fe(0) corroded by hydrogenase-positive microbes.

Therefore, we evaluated the possibility of anaerobic microbial stainless steel corrosion either with H_2 as an electron carrier, or via direct iron-to-microbe electron transfer, with genetically modified strains of *G. sulfurreducens* as well as wild-type *Geobacter metallireducens*, a species that is unable to use H_2 [26]. The results suggest that H_2 is unlikely to be an effective electron shuttle for microbial corrosion of stainless steel. However, microbial corrosion of stainless steel via direct iron-to-microbe electron transfer is possible.

Materials and methods

Materials

A 316L stainless steel (elemental composition (wt %): 0.021 C, 0.43 Si, 1.18 Mn, 16.78 Cr, 2.09 Mo, 0.0006 S, 0.032 P, 10.5 Ni, balance Fe) was supplied by the Institute of Metal Research, Chinese Academy of Sciences (Shenyang, China). The stainless steel was cut into coupons (10 mm × 10 mm × 5 mm), the surfaces abraded with three different grades of sandpaper (220, 600, and 1200 grits), washed with 100% ethanol, and air-dried. For electrochemical tests, the coupons were connected with rubber-coated copper wire and sealed with an epoxy resin to expose a surface area of 1 cm^2. Prior to each experiment, the electrodes and coupons were sterilized in 75% (v/v) ethanol and dried in a UV chamber (XL-1500 Series UV Crosslinker, SPECTRONICS, New York, USA) for 30 min.

Bacterial strains and growth condition

G. sulfurreducens [27] and *G. metallireducens* [26, 28] strains were obtained from the Lovley lab culture collection. The following mutant strains were constructed as previously described: *G. sulfureducens* strain ACL [29], *G. sulfurreducens* strain ACL_{HF} [11], *G. sulfurreducens* strain ACL_{HF} Δ*omcS* [11], *G. sulfurreducens* strain ACL_{HF}Δ*omcS* complemented with expression of *omcS in trans* [11], and *G. metallireducens* ΔGmet 1868 [30].

All *G. sulfurreducens* strains were routinely maintained under strict anaerobic conditions at 30 °C in freshwater medium [31] (per liter: 2.5 g $NaHCO_3$, 0.25 g NH_4Cl, 0.6 g $NaH_2PO_4{\cdot}H_2O$, 0.1 g KCl), amended with 10 ml DL vitamins [27], 10 ml DL minerals [27], with acetate (20 mM) as the electron donor and fumarate (40 mM) as the electron acceptor. *G. metallireducens* strains were maintained in the freshwater medium with acetate (10 mM) as the electron donor and nitrate (5 mM) as the electron acceptor. Analyses of growth, H_2 production, and pitting of stainless steel were conducted in 50 ml of medium in 160 ml serum bottles that were sealed with butyl rubber stoppers. Coupons of 316L stainless steel were provided as the sole electron donor. Fumarate (40 mM) was the sole electron acceptor for studies with *G. sulfurreducens*. Nitrate (5 mM) was the electron acceptor for *G. metallireducens*.

For electrochemical tests, once cultures reached an OD_{600} of 0.5, 50 ml was inoculated into electrochemical cells filled with 250 ml freshwater medium with fumarate (40 mM) or nitrate (5 mM) as the electron acceptor for *G. sulfurreducens* or *G. metallireducens*, respectively.

Electrochemical tests

Electrochemical studies were carried out in a three-electrode glass cell containing 300 ml of culture medium incubated anaerobically at 25 °C. A 316L stainless steel electrode served as the working electrode, the counter electrode was platinum, and the reference electrode consisted of a saturated calomel electrode. All open circuit potential (OCP), linear polarization resistance (LPR), electrochemical impedance spectroscopy (EIS), and potential dynamic polarization measurements were obtained with a potentiostat (G300, Gamry Instrument, USA). LPR tests were recorded at a scan rate of 0.125 mV s^{-1} in the range of −5 to 5 mV versus E_{OCP}. EIS was performed under a steady-state E_{OCP} using a 5 mV amplitude sinusoidal wave in the frequency range of 10,000–0.01 Hz. Before the potentiodynamic polarization scans, the electrodes were in the open circuit mode until a steady free OCP was reached. The polarization curves were performed at a scan rate of 0.5 mV s^{-1} from −0.5 to 2 V versus E_{OCP}. Each electrochemical test was conducted in triplicate in three separate experiments to ensure reproducibility.

Analytical techniques

Succinate production was monitored over time with a Shimadzu high-performance liquid chromatograph outfitted with an Aminex HPX-87H ion exclusion column (300 mm by 7.8 mm) and 0.5 ml min^{-1} eluent of 8.0 mM sulfuric acid, as previously described [32]. pH values were determined with a pH meter (UltraBASIC UB-5, Denver Instrument, USA).

Hydrogen in the headspace of cultures was measured with a trace analytical instrument (ta3000 gas analyzer, AMETEK, USA). The reduction gas detection (RGD) bed was filled with mercuric oxide (HgO). The RGD bed temperature was set to 285 °C, and the RGD column temperature 105 °C. The carrier gas was N_2 at 80 psi. The lower and upper detection limits for the instrument were 1 part per billion and 3 parts per million by volume, respectively.

Surface analysis

After incubation, coupons were gently rinsed with 0.1 M phosphate buffer (pH 7.2) and fixed with 2.5% (v/v) glutaraldehyde overnight at 4 °C. The coupons were then washed three times in the phosphate buffer and then dehydrated with a graded series (35, 50, 70, 80, 90, 95, and 100% v/v) of ethanol solutions for 10 min each. Anhydrous ethanol dehydration was repeated three times. scanning electron microscopy (SEM) was conducted with an ultrahigh-resolution field emission scanning electron microscope (FEI Magellan 400; Nanolab Technologies, CA, USA).

To observe corrosion pits underneath biofilms, coupons were first cleaned with Clarke's solution (strong hydrochloric acid combined with antimony chloride and stannous chloride prepared as previously described [33]) to remove corrosion products and biofilms on coupon surfaces. Pit depth was measured with a Nikon A1 Resonant Scanning Confocal Microscope with Structured Illumination Super-Resolution (Nikon Instruments Inc., Japan).

Biofilms on coupons were stained with LIVE/DEAD BacLight Bacterial Viability Kit (Invitrogen, USA). The kit has two fluorescent dyes, the green-fluorescent SYTO-9 dye designed to measure live cells and the red-fluorescent propidium iodide (PI) dye designed to measure dead cells. After staining, samples were observed under CLSM at two wavelengths (488 nm for dye SYTO-9 and 559 nm for dye PI). Cell numbers in the 3D scanned images were calculated with NIS-Elements software (https://www.nikonmetrology.com/en-us/product/nis-elements-microscope-imaging-software).

Data analysis

All the experiments were conducted in triplicate and each experiment was repeated at least three times. Each data point was the result from a single test of each device. Uncertainty in a reported measurement was expressed by standard error. P value was determined to compare the differences between each group. Results were considered significantly different for P value < 0.05.

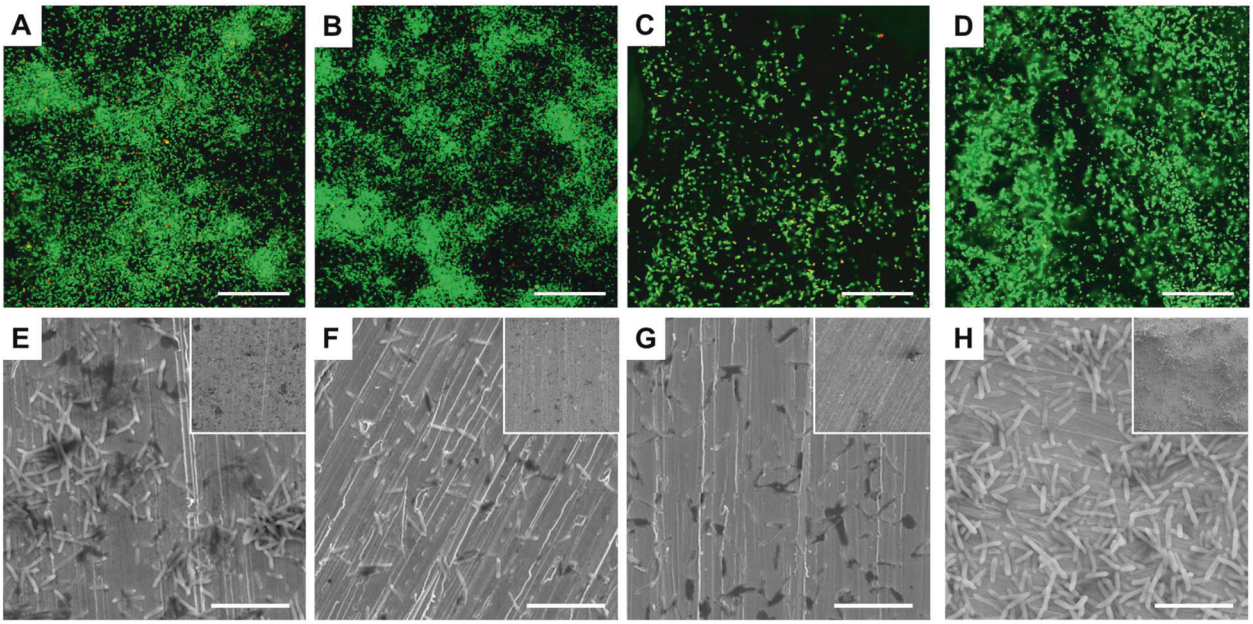

Fig. 1 Biofilm formation on stainless steel after 7 days. Confocal scanning laser microscopy (CLSM) images (scale bar = 50 µm) of biofilms attached to stainless steel after the surface was treated with live/dead stain: **A** strain ACL; **B** strain ACL_{HF}; **C** strain $ACL_{HF}\Delta omcS$. **D** Strain in which $ACL_{HF}\Delta omcS$ was complemented by expressing *omcS in trans*. High magnification (main image) and lower magnification (upper right insert) scanning electron microscope images (scale bar = 5 µm) of the following biofilms: **E** strain ACL; **F** strain ACL_{HF}; **G** strain $ACL_{HF}\Delta omcS$; **H** strain in which $ACL_{HF}\Delta omcS$ was complemented by expressing *omcS in trans*.

Results and discussion

Growth of *G. sulfurreducens* strains on stainless steel

Over 7 days, both strain ACL (Fig. 1A, E), which can grow with H_2 or formate as the electron donor, and strain ACL_{HF} (Fig. 1B, F), which is unable to use H_2 or formate, grew as biofilms on stainless steel. Cell growth was accompanied with the reduction of fumarate to succinate (Fig. 2). As expected from previous studies with Fe(0) [11], there was no turbidity in the stainless steel cultures of strain ACL_{HF} (Supplementary Fig. S1), which has to rely on direct iron-to-microbe electron transfer. In previous studies with Fe(0), strain ACL primarily grew on the H_2 evolved from Fe(0), producing substantial culture turbidity attributable to planktonic cell growth on H_2 [11]. However, there was no turbidity in cultures of strain ACL growing on stainless steel (Supplementary Fig. S1).

The lack of planktonic growth of strain ACL suggested that, unlike Fe(0), the stainless steel was not generating sufficient H_2 to support the growth of planktonic cells. Direct measurements revealed that the concentration of H_2 in abiotic controls (approximately 0.1 Pa) containing stainless steel were 50,000-fold lower than comparable abiotic controls with Fe(0), demonstrating that there was little, if any, production of H_2 from stainless steel (Fig. 3). This finding was consistent with electrochemical measurements,

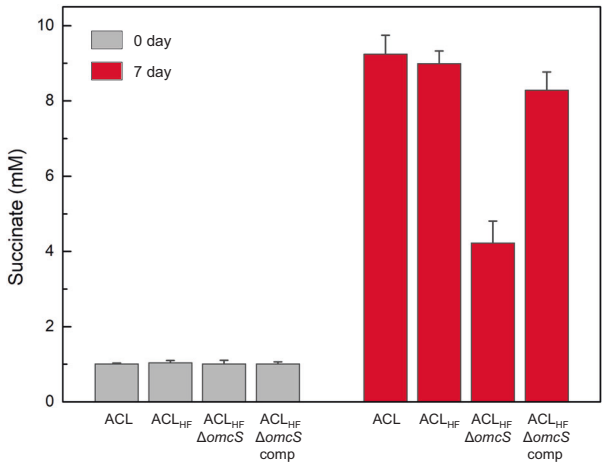

Fig. 2 Concentrations of succinate, the end product of fumarate reduction, at the beginning and end of the 7-day incubation. The abbreviation comp represents complementation with the expression of *omcS in trans*. Results are the mean and standard deviation ($n = 3$).

discussed later, that demonstrated that H_2 production was thermodynamically unfavorable in both the abiotic control and in the presence of strain ACL and ACL_{HF}. H_2 levels in cultures of strain ACL with stainless steel were comparable to those of the abiotic control, indicating that even though strain ACL can grow on H_2, it was unable to consume H_2 at the low concentrations available. These results suggested that strain ACL relied on direct electron uptake when grown on stainless steel.

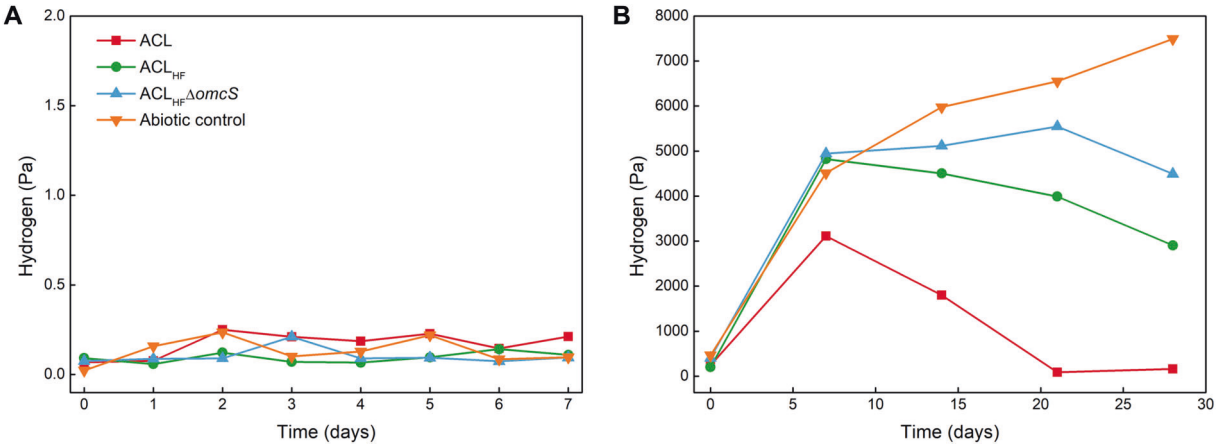

Fig. 3 Stainless steel yields much less H_2 than Fe(0). H_2 concentration in the headspace in the presence of stainless steel (**A**) or Fe (0) (**B**). Note the differences in units on the *y*-axis in the two panels. Data in (**B**) from reference [11]. Results are the mean and standard deviation ($n = 3$).

A strain in which the gene for the outer-surface cytochrome OmcS was deleted from strain ACL_{HF} (ACL_{HF}-Δ*omcS*) cell grew much less on the stainless steel than strain ACL_{HF} (Fig. 1C, G) and reduced about 60% less fumarate to succinate (Fig. 2). Expression of *omcS in trans* restored the capacity for growth on the stainless steel (Fig. 1D, H) and fumarate reduction (Fig. 2). This result is consistent with the previous finding that OmcS is an important component for direct electron uptake from Fe(0) [11]. Deletion of OmcS did not completely inhibit growth on stainless steel, presumably because *G. sulfurreducens* has multiple outer-surface electrical contacts [34–36] that would all need to be deleted to completely inhibit extracellular electron exchange.

The pH of the culture medium in the biotic incubations and the abiotic control was 7.0 ± 0.1 after 7 days, which was statistically equivalent to the initial pH (6.9 ± 0.1) measured at the time of inoculation. These results ruled out pH changes as a potential explanation for the corrosion observed.

Pitting

In order to determine whether growth on the stainless steel surface resulted in pitting, the biofilms and corrosion products were removed with an acidic solution after 7 days of incubations. The stainless steel surfaces of abiotic controls were relatively smooth (Fig. 4A, F) and the few pits that were observed were relatively shallow (Fig. 4K). The average depth of the ten largest pits was only 0.9 ± 0.4 µm. In contrast, large and deep pits were visible on stainless steel incubated in the presence of strains ACL and ACL_{HF} (Fig. 4B, C, G, H, K, L). Consistent with its poor growth on stainless steel, the pit depths associated with strain ACL_{HF}Δ*omcS* were much smaller than for strain ACL_{HF} (Fig. 4D, I), the average depth of ten largest pits was 1.6 ± 0.5 µm (Fig. 4K) with average diameter of 3.8 ± 1.0 µm (Fig. 4L). Complementation of ACL_{HF}Δ*omcS* with expression of *omcS in trans* restored higher corrosion rates with a pit size comparable with strains ACL and ACL_{HF} (Fig. 4E, J, K, L).

A similar pattern of corrosion was observed from quantifying the abundance of pits on the stainless steel surface (Fig. 4M). The pit density of the abiotic control (24 ± 15 pits mm^{-2}) was much less than for strains ACL and ACL_{HF} (110 ± 28 and 126 ± 20 pits mm^{-2}, respectively). When *omcS* was deleted from strain ACL_{HF}, the pit density decreased to 40 ± 17 pits mm^{-2}. Complementation of the *omcS* mutation increased the pit density to 85 ± 18 pits mm^{-2}.

Electrochemical analysis of corrosion

Several classical electrochemical methods further demonstrated that strain ACL and strain ACL_{HF} actively corroded stainless steel and that the presence of an uptake hydrogenase did not enhance the corrosion capacity of strain ACL over strain ACL_{HF}. The lowest OCP for the stainless steel in the abiotic control was 160.9 mV_{SHE} (Fig. 5A), much more electropositive than the midpoint potential for H_2 evolution under the conditions (pH 7, 25 °C, 0.1 Pa) in the culture medium:

$$2H^+ + 2e^- \rightleftarrows H_2 (-236.2\ mV_{SHE}) \quad (2)$$

Thus, H_2 formation was thermodynamically unfavorable, explaining the observed lack of H_2 production.

In contrast, the OCP of the stainless steel colonized by strains ACL and ACL_{HF} was much lower than the abiotic control, stabilizing at approximately −141.4 and −116.6 mV_{SHE}, respectively (Fig. 5A). This low potential

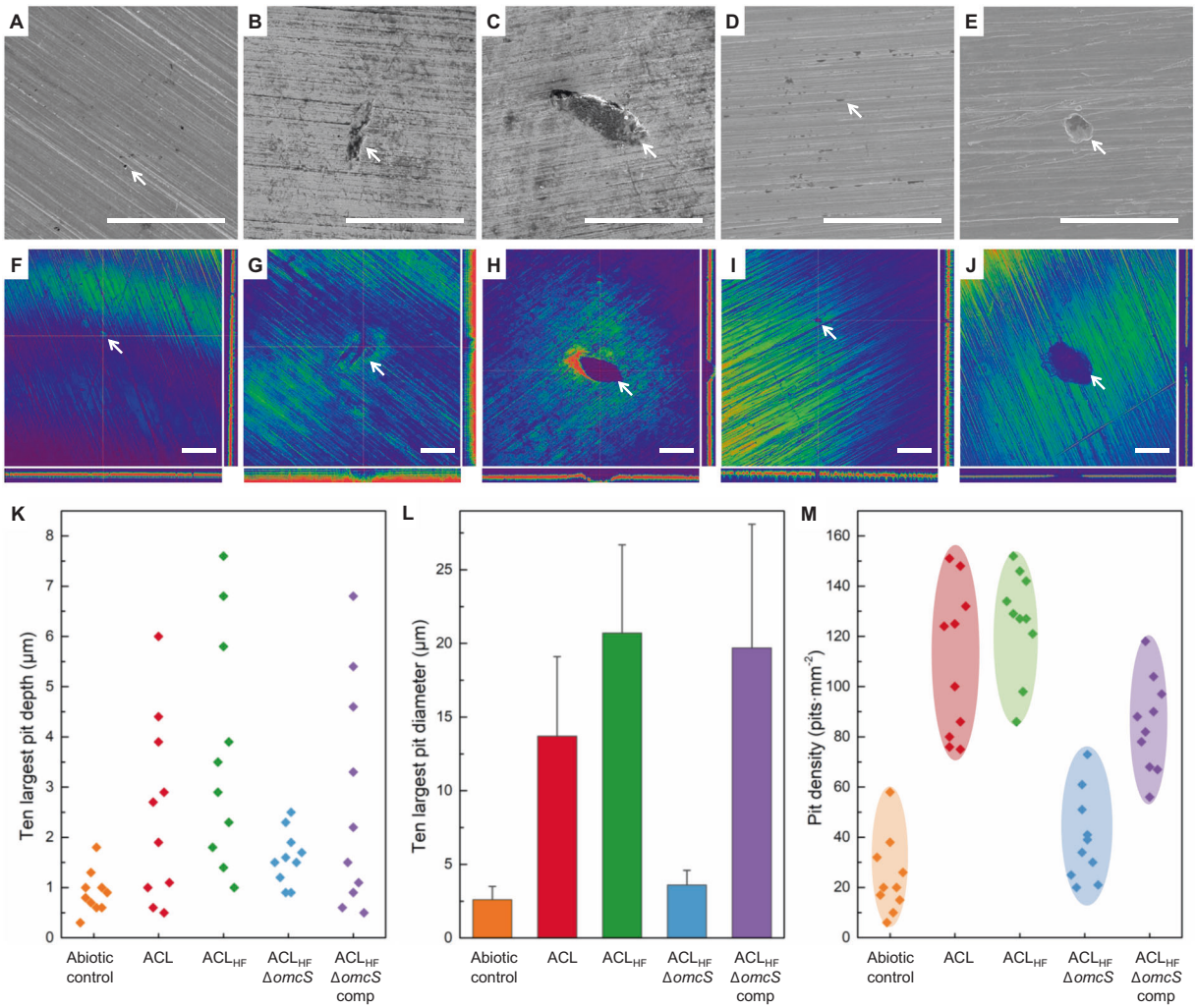

Fig. 4 Visualization of pitting on stainless steel. Scanning electron micrographs of stainless steel surfaces (scale bar = 50 μm) in: **A** abiotic control; **B** strain ACL; **C** strain ACL$_{HF}$; and **D** strain ACL$_{HF}$Δ*omcS*. **E** Strain in which ACL$_{HF}$Δ*omcS* was complemented by expressing *omcS in trans*. Scale bar = 50 μm. Confocal scanning laser microscopy images of stainless steel surfaces: **F** abiotic control; **G** strain ACL; **H** strain ACL$_{HF}$; **I** strain ACL$_{HF}$Δ*omcS*; **J** strain in which ACL$_{HF}$Δ*omcS* was complemented by expressing *omcS in trans*. Analysis of **K** pit depth and **L** pit diameter for the ten largest pits as well as **M** pit density (data from ten random fields (0.1 mm^2) examined on each of five coupons for each treatment; mean ± standard deviation).

indicated that release of electrons from the stainless steel was much more favorable in the presence of the strain ACL and ACL$_{HF}$ biofilms, consistent with the high rates of corrosion associated with these biofilms. However, that was still too electropositive to support H_2 production (reaction 2), consistent with the lack of H_2 accumulation in the strain ACL$_{HF}$ cultures and the lack of planktonic growth of strain ACL.

The OCP for the stainless steel in the presence of strain ACL$_{HF}$Δ*omcS* was intermediate between the abiotic control and the stainless steel colonized by the strain ACL and ACL$_{HF}$ biofilms (Fig. 5A), in accordance with the low rates of corrosion in those samples. When the *omcS* deletion was complemented the OCP was comparable to the wild-type control (Fig. 5A).

Several other electrochemical techniques for corrosion characterization also signified higher rates of corrosion in the presence of strains ACL and ACL$_{HF}$ and reduced corrosion in the absence of OmcS. For example, LPR (R_p) is inversely proportional to the corrosion rate [37]. $1/R_p$ was low in the abiotic control, further demonstrating that the medium was not corrosive (Fig. 5B). There was more variability in the $1/R_p$ of culture replicates of strain ACL$_{HF}$ than strain ACL. The $1/R_p$ of strain ACL was stable at around 0.009 $k\Omega^{-1}\cdot cm^{-2}$, whereas strain ACL$_{HF}$ had a range from 0.012 to 0.029 $k\Omega^{-1}\cdot cm^{-2}$. The mean values for two strains were not statistically significantly different. Both had $1/R_p$ values that were more than five-fold higher than the abiotic control (Fig. 5B). Strain ACL$_{HF}$Δ*omcS* was comparable to the abiotic control, consistent with the other

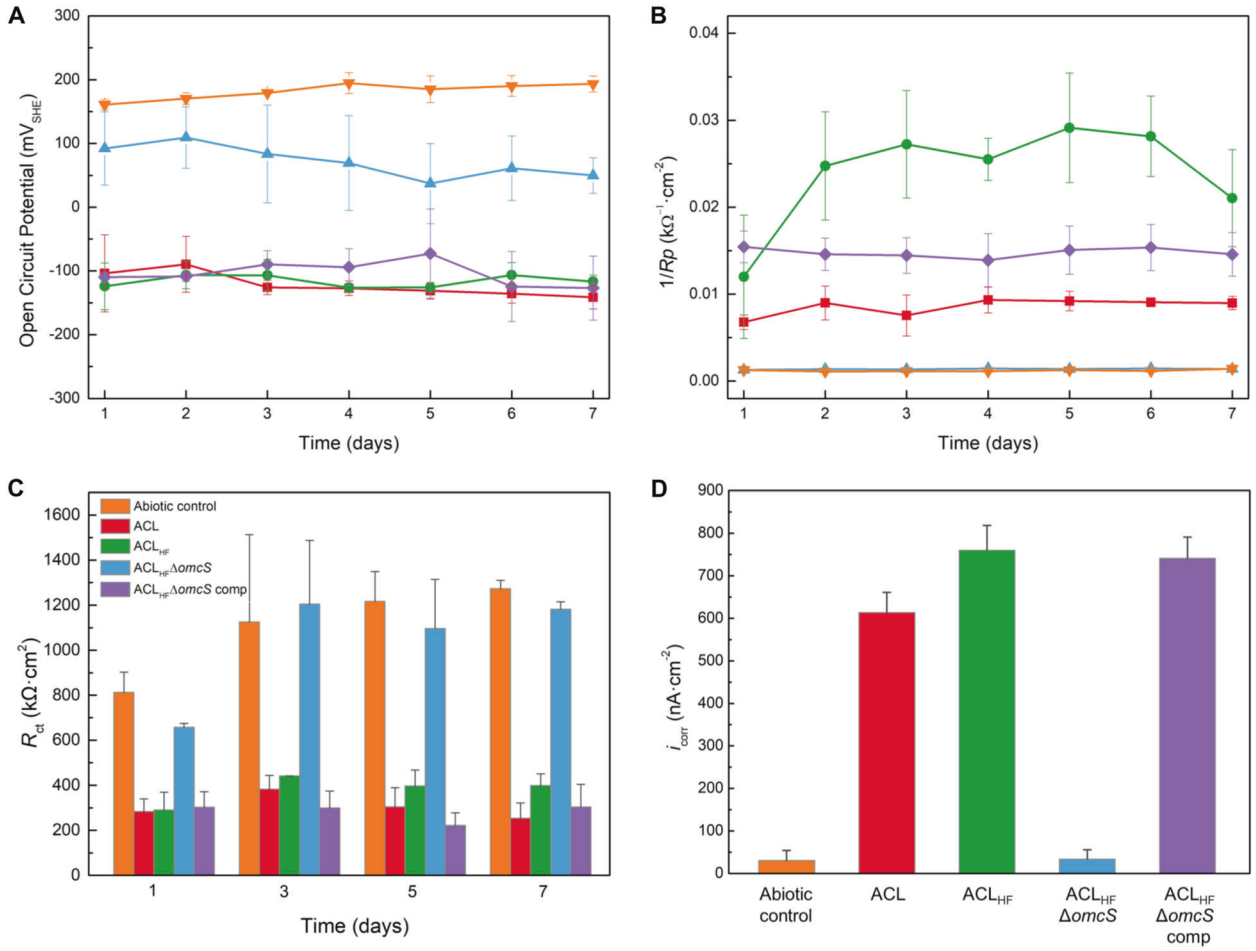

Fig. 5 Electrochemical analysis of stainless steel. A Open circuit potential over time. **B** $1/R_p$ over time. **C** R_{ct} over time (obtained from EIS data, Supplementary Table S1). **D** Corrosion current density after 7 days. ACL, ACL_{HF}, $ACL_{HF}\Delta omcS$, Strain in which $ACL_{HF}\Delta omcS$ was complemented by expressing *omcS in trans*, and abiotic control. Results are the mean and standard deviation ($n = 3$).

results indicative of slow corrosion with this strain. Complementation restored $1/R_p$ to a level found in the ACL_{HF} strain (Fig. 5B).

Modeling of EIS data (Supplementary Figs. S2 and S3 and Supplementary Table S1) indicated that charge transfer resistance between the biofilm and the stainless steel matrix, designated R_{ct}, was much higher in the abiotic control and strain $ACL_{HF}\Delta omcS$ than for strain ACL and strain ACL_{HF} (Fig. 5C). The charge transfer resistance for strain ACL was not statistically significantly different than for strain ACL_{HF}, further demonstrating that the elimination of hydrogenase activity did not impact corrosion.

A measure of corrosion current density, designated i_{corr} (Fig. 5D), which is directly proportional to the corrosion rate, can be derived from potentiodynamic polarization curves (Supplementary Fig. S4) [38]. The i_{corr} for the abiotic control and strain $ACL_{HF}\Delta omcS$ were similar, about 32 ± 23 nA·cm^{-2}, and significantly lower than the i_{corr} for strain ACL (614 ± 47 nA·cm^{-2}), strain ACL_{HF} (760 ± 58 nA·cm^{-2}), and the *omcS* complemented strain of strain $ACL_{HF}\Delta omcS$ (741 ± 50 nA·cm^{-2}) (Fig. 5D). These results further demonstrate the importance of OmcS in the corrosion. The differences in corrosion between strains with and without OmcS could not be attributed to the difference in the number of cells colonizing the stainless steel surface because normalization for cell numbers to calculate i_{corr}/cell and R_{ct}/cell continued to indicate reduced corrosion in the absence of OmcS (Supplementary Fig. S5).

Direct metal-microbe electron transfer with *G. metallireducens*

G. metallireducens, which is unable to utilize H_2 [26], but is capable of directly receiving electrons from electrodes to support nitrate reduction [39], heavily colonized stainless steel in medium with nitrate provided as an electron acceptor (Fig. 6A). This was accompanied with the reduction of nitrate (Fig. 6C) and obvious pitting (Fig. 6D, E). The corrosion mechanism was further evaluated with a strain of *G.*

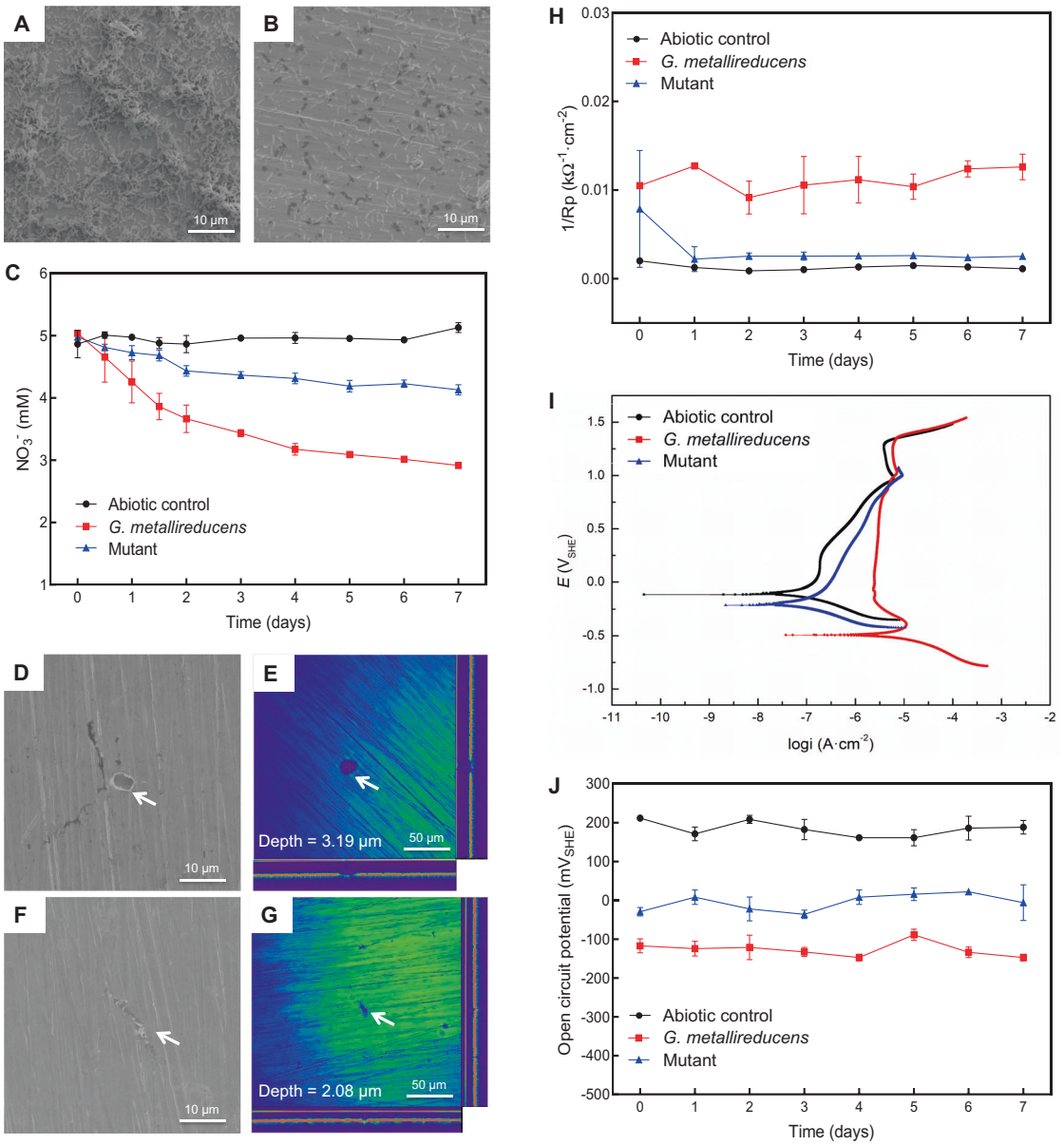

Fig. 6 *G. metallireducens* required an outer-membrane cytochrome to corrode stainless steel. Scanning electron micrographs of biofilm formation on stainless steel after 7 days of wild-type (**A**) and a mutant strain in which the *c*-type cytochrome Gmet 1868 was deleted (**B**). **C** Nitrate concentrations over time. Scanning electron micrographs (**D**, **F**) and confocal scanning laser micrographs (**E**, **G**) of pits on stainless steel after 7 days for wild-type (**D**, **E**), and cytochrome mutant strain (**F**, **G**). **H** $1/R_p$ over time. **I** Potentiodynamic polarization curves after 7 days of incubation. **J** Open circuit potential over time.

metallireducens in which the gene Gmet 1868 was deleted. This gene encodes a multi-heme *c*-type cytochrome that is important for extracellular electron exchange [30, 40]. The cytochrome-deficient mutant only lightly colonized the stainless steel surface (Fig. 6B) with minimal pitting (Fig. 6F, G) and nitrate reduction (Fig. 6C). The greater corrosivity of the wild-type strain was apparent from electrochemical data (Fig. 6H, I). The $1/R_p$ (ca. 0.01 $k\Omega^{-1}\cdot cm^{-2}$; Fig. 6H) and i_{corr} (1098 ± 87 $nA\cdot cm^{-2}$; Fig. 6I) of the wild-type strain were much higher than those of the cytochrome-deficient mutant, which had values ($1/R_p$ (ca. 0.003 $k\Omega^{-1}\cdot cm^{-2}$; Fig. 6H and i_{corr} 101 ± 22 $nA\cdot cm^{-2}$; Fig. 6I)) similar to those of the uninoculated control. The wild-type also achieved a much lower OCP (Fig. 6J). These results demonstrated that cytochrome Gmet 1868 is important for electron uptake from stainless steel. However, like *G. sulfurreducens*, *G. metallireducens* is likely to express multiple electrical connects on its outer surface that would all need to be deleted in order to completely prevent electron uptake from stainless steel.

Implications

The results demonstrate that microbial corrosion of stainless steel, a common structural material, is possible, but in contrast to corrosion of pure Fe(0), H_2 is unlikely to serve as an intermediary electron carrier. This distinction between corrosion of stainless steel and pure Fe(0) is significant because prior studies on the mechanisms for microbial iron corrosion have focused on pure Fe(0) [5, 7, 8, 10, 12, 16], which unlike stainless steel, readily evolves H_2 and is not a common structural material. Even microbes capable of direct electron uptake may favor H_2 uptake as their primary route for Fe(0) corrosion if they possess uptake hydrogenases [11]. These results suggest that future corrosion studies should focus on actual iron materials rather than pure Fe(0) in order to develop corrosion models and mitigation strategies for economically important iron materials.

Outside of artificial laboratory studies, the microorganisms that are actually responsible for accelerating the corrosion of iron-containing metals and their mechanisms for gaining electrons from Fe(0) are poorly understood [23]. The finding that multi-heme *c*-type cytochromes, a common feature of many electroactive microbes, can be associated with direct iron-to-microbe electron transfer ([11] and this study) provides an important molecular target to hunt for such microbes.

Acknowledgements We thank James J. Chambers of UMass Amherst Life Sciences Laboratories' Light Microscopy Core for facilitating CLSM and image analysis, and Louis E. Raboin of UMass Amherst Electron Microscopy Center for facilitating SEM. This work was supported by grants to DX from the National Natural Science Foundation of China (Nos. U2006219 and 51871050), the National Key Research and Development Program of China (2020YFA0907300), the Fundamental Research Funds for the Central Universities (Nos. N180203019 and N2002019), and Liaoning Revitalization Talents Program (No. XLYC1907158).

Author contributions H-YT, DX, FW, and DRL designed the research. H-YT, CY, DEH, TU, and CCP conducted the experiments and analyses. TLW performed the HPLC experiment and data analysis. All authors contributed to data interpretation, writing, and editing of the manuscript.

Compliance with ethical standards

Conflict of interest The authors declare no competing interests.

Publisher's note Springer Nature remains neutral with regard to jurisdictional claims in published maps and institutional affiliations.

References

1. Skovhus TL, Eckert RB, Rodrigues E. Management and control of microbiologically influenced corrosion (MIC) in the oil and gas industry—overview and a North Sea case study. J Biotechnol. 2017;256:31–45.
2. Procopio L. The era of 'omics' technologies in the study of microbiologically influenced corrosion. Biotechnol Lett. 2020;42:341–56.
3. Gu T, Jia R, Unsal T, Xu D. Toward a better understanding of microbiologically influenced corrosion caused by sulfate reducing bacteria. J Mater Sci Technol. 2019;35:631–6.
4. Gaines RH. Bacterial activity as a corrosive influence in the soil. Ind Eng Chem. 1910;2:128–30.
5. Philips J. Extracellular electron uptake by acetogenic bacteria: Does H_2 consumption favor the H_2 evolution reaction on a cathode or metallic iron? Front Microbiol. 2020;10:2997.
6. Daniels L, Belay N, Rajagopal BS, Weimer PJ. Bacterial methanogenesis and growth from CO_2 with elemental iron as the sole source of electrons. Science. 1987;237:509–11.
7. Deutzmann JS, Sahin M, Spormann AM. Extracellular enzymes facilitate electron uptake in biocorrosion and bioelectrosynthesis. mBio. 2015;6:e00496–15.
8. Philips J, Monballyu E, Georg S, De Paepe K, Prevoteau A, Rabaey K, et al. An *Acetobacterium* strain isolated with metallic iron as electron donor enhances iron corrosion by a similar mechanism as *Sporomusa sphaeroides*. FEMS Microbiol Ecol. 2019;95:fiy222.
9. Tsurumaru H, Ito N, Mori K, Wakai S, Uchiyama T, Iino T, et al. An extracellular [NiFe] hydrogenase mediating iron corrosion is encoded in a genetically unstable genomic island in *Methanococcus maripaludis*. Sci Rep. 2018;8:1–10.
10. Philips J, Van den Driessche N, De Paepe K, Prévoteau A, Gralnick JA, Arends JBA, et al. A novel *Shewanella* isolate enhances corrosion by using metallic iron as the electron donor with fumarate as the electron acceptor. Appl Environ Microbiol. 2018;84:e01154–18.
11. Tang H-Y, Holmes DE, Ueki T, Palacios PA, Lovley DR. Iron corrosion via direct metal-microbe electron transfer. mBio. 2019;10:e00303–19.
12. Dinh HT, Kuever J, Mußmann M, Hassel AW, Stratmann M, Widdel F. Iron corrosion by novel anaerobic microorganisms. Nature. 2004;427:829–32.
13. Kato S. Microbial extracellular electron transfer and its relevance to iron corrosion. Micro Biotechnol. 2016;9:141–8.
14. Enning D, Garrelfs J. Corrosion of iron by sulfate-reducing bacteria: new views of an old problem. Appl Environ Microbiol. 2014;80:1226–36.
15. Lovley DR. Powering microbes with electricity: direct electron transfer from electrodes to microbes. Environ Microbiol Rep. 2011;3:27–35.
16. Palacios PA, Snoeyenbos-West O, Loscher CR, Thamdrup B, Rotaru AE. Baltic Sea methanogens compete with acetogens for electrons from metallic iron. ISME J. 2019;13:3011–23.
17. Yu L, Duan J, Du X, Huang Y, Hou B. Accelerated anaerobic corrosion of electroactive sulfate-reducing bacteria by electrochemical impedance spectroscopy and chronoamperometry. Electrochem Commun. 2013;26:101–4.
18. Xu D, Li Y, Song F, Gu T. Laboratory investigation of microbiologically influenced corrosion of C1018 carbon steel by nitrate reducing bacterium *Bacillus licheniformis*. Corros Sci. 2013;77:385–90.
19. Xu D, Gu T. Carbon source starvation triggered more aggressive corrosion against carbon steel by the *Desulfovibrio vulgaris* biofilm. Int Biodeterior Biodegrad. 2014;91:74–81.
20. Venzlaff H, Enning D, Srinivasan J, Mayrhofer KJJ, Hassel AW, Widdel F, et al. Accelerated cathodic reaction in microbial corrosion of iron due to direct electron uptake by sulfate-reducing bacteria. Corros Sci. 2013;66:88–96.
21. Vigneron A, Head IM, Tsesmetzis N. Damage to offshore production facilities by corrosive microbial biofilms. Appl Microbiol Biotechnol. 2018;102:2525–33.

22. Sharma M, Bajracharya S, Gildemyn S, Patil SA, Alvarez-Gallego Y, Pant D, et al. A critical revisit of the key parameters used to describe microbial electrochemical systems. Electrochim Acta. 2014;140:191–208.
23. Lekbach Y, Liu T, Li Y, Moradi M, Dou W, Xu D, et al. Microbial corrosion of metals-the corrosion microbiome. *Adv Microb Physiol*. 2021;78. https://doi.org/10.1016/bs.ampbs.2021.01.002.
24. Iannuzzi M, Barnoush A, Johnsen R. Materials and corrosion trends in offshore and subsea oil and gas production. npj Mater Degrad. 2017;1:2.
25. Ohmi T, Nakagawa Y, Nakamura M, Ohki A, Koyama T. Formation of chromium oxide on 316L austenitic stainless steel. J Vac Sci Technol A. 1996;14:2505–10.
26. Lovley DR, Giovannoni SJ, White DC, Champine JE, Phillips E, Gorby YA, et al. *Geobacter metallireducens* gen. nov. sp. nov., a microorganism capable of coupling the complete oxidation of organic compounds to the reduction of iron and other metals. Arch Microbiol. 1993;159:336–44.
27. Caccavo F, Lonergan DJ, Lovley DR, Davis M, Stolz JF, McInerney MJ. *Geobacter sulfurreducens* sp. nov., a hydrogen- and acetate-oxidizing dissimilatory metal-reducing microorganism. Appl Environ Microbiol. 1994;60:3752–9.
28. Lovley DR, Stolz JF, Nord GL, Phillips EJ. Anaerobic production of magnetite by a dissimilatory iron-reducing microorganism. Nature. 1987;330:252–4.
29. Ueki T, Nevin KP, Woodard TL, Aklujkar MA, Holmes DE, Lovley DR. Construction of a *Geobacter* strain with exceptional growth on cathodes. Front Microbiol. 2018;9:1512.
30. Smith JA, Lovley DR, Tremblay P-L. Outer cell surface components essential for Fe (III) oxide reduction by *Geobacter metallireducens*. Appl Environ Microbiol. 2013;79:901–7.
31. Lovley DR, Phillips EJ. Novel mode of microbial energy metabolism: organic carbon oxidation coupled to dissimilatory reduction of iron or manganese. Appl Environ Microbiol. 1988;54:1472–80.
32. Nevin KP, Richter H, Covalla S, Johnson J, Woodard T, Orloff A, et al. Power output and columbic efficiencies from biofilms of *Geobacter sulfurreducens* comparable to mixed community microbial fuel cells. Environ Microbiol. 2008;10:2505–14.
33. ASTM G1-03. Standard practice for preparing, cleaning, and evaluation corrosion test specimens. ASTM International. 2003.
34. Lovley DR, Ueki T, Zhang T, Malvankar NS, Shrestha PM, Flanagan KA. et al. *Geobacter*: the microbe electric's physiology, ecology, and practical applications. Adv Microb Physiol. 2011;59:1–100.
35. Ueki T, DiDonato LN, Lovley DR. Toward establishing minimum requirements for extracellular electron transfer in *Geobacter sulfurreducens*. FEMS Microbiol Lett. 2017;364:fnx093.
36. Voordeckers JW, Kim B-C, Izallalen M, Lovley DR. Role of *Geobacter sulfurreducens* outer surface c-type cytochromes in reduction of soil humic acid and anthraquinone-2, 6-disulfonate. Appl Environ Microbiol. 2010;76:2371–5.
37. Durrani F, Wesley R, Srikandarajah V, Eftekhari M, Munn S. Predicting corrosion rate in chilled HVAC pipe network: coupon vs linear polarisation resistance method. Eng Fail Anal. 2020;109:104261.
38. McCafferty E. Validation of corrosion rates measured by the Tafel extrapolation method. Corros Sci. 2005;47:3202–15.
39. Gregory KB, Bond DR, Lovley DR. Graphite electrodes as electron donors for anaerobic respiration. Environ Microbiol. 2004;6:596–604.
40. Rotaru AE, Shrestha PM, Liu F, Shrestha M, Shrestha D, Embree M, et al. A new model for electron flow during anaerobic digestion: direct interspecies electron transfer to *Methanosaeta* for the reduction of carbon dioxide to methane. Energy Environ Sci. 2014;7:408–15.